Kinetic Mechanism of Kinesin Motor Domain†

Yong-Ze Ma and Edwin W. Taylor*

Department of Molecular Genetics and Cell Biology, The University of Chicago, Cummings Life Science Center, 920 East 58 Street, Chicago, Illinois 60637

Received March 8, 1995; Revised Manuscript Received June 9, 1995®

ABSTRACT: The kinetic mechanism of the human kinesin ATPase motor domain K379, expressed in *Escherichia coli*, was determined by transient and steady-state kinetic studies. The steps in nucleotide binding were measured using the fluorescent substrate analogues, methylanthraniloyl ATP (mant-ATP) and mant-ADP. Both nucleotides gave a two-step fluorescence signal, an increase followed by a decrease, which indicates that two isomerizations are induced by nucleotide binding. The ATPase mechanism is fitted by a six-step reaction: $K + T \overset{1}{\rightleftharpoons} K(T) \overset{2}{\rightleftharpoons} K{\cdot}T \overset{3}{\rightleftharpoons} K{\cdot}D{\cdot}P \overset{4(-P)}{\rightleftharpoons} K{\cdot}D \overset{5}{\rightleftharpoons} K(D) \overset{6}{\rightleftharpoons} K + D$ where, T, D, and P refer to nucleotide triphosphate, nucleotide diphosphate, and inorganic phosphate, respectively; K(T) and K(D) are states in rapid equilibrium with the free nucleotide. A set of kinetic constants for 20 °C 50 mM NaCl is $K_1 = 2 \times 10^4$ M^{-1}, $k_2 = 200$ s^{-1}, $k_3 = 9$ s^{-1}, $k_5 = 0.01$ s^{-1}, and $K_6 = 2 \times 10^{-5}$ M. Values of K_1 and K_6 are estimates for mant-ATP and mant-ADP, respectively. ADP dissociation is the rate-limiting step. The rate constant for a decrease in fluorescence for the transitions from the high fluorescence K·T state to the low fluorescence K·D state is equal to k_3, the rate constant of the hydrolysis step measured by quench flow experiments. The decrease could occur in step 3 or step 4 if $k_4 > k_3$. The binding of mant-ADP fitted the scheme $K + D \overset{K_a}{\rightleftharpoons} K(D) \overset{k_b}{\rightleftharpoons} K{\cdot}D_1 \overset{k_c}{\rightleftharpoons} K{\cdot}D_2$ where $K_a = (1/K_6) = 5 \times 10^4$ M^{-1}; $k_b = 200$ s^{-1} is the rate constant of the transition to the high fluorescence K·D$_1$ state; $k_c = 40$ s^{-1} is the rate of the transition to the low fluorescence K·D$_2$ state (in 50 mM NaCl). The final level of enhancement is the same for mant-ADP and mant-ATP in the steady state, and the K·D$_2$ and K·D states have the same rate constant of mant ADP dissociation and are considered to be identical. The rate constants agreed closely with values obtained previously for the kinesin tetramer prepared from calf brain [Sadhu, A., & Taylor, E. W. (1992) *J. Biol. Chem. 267*, 11352−11359].

The kinetic mechanism of kinesin ATPase prepared from brain has been studied by steady-state and transient kinetic methods. The enzyme shows an initial burst of ATP hydrolysis and dissociation of phosphate followed by a smaller rate for ADP dissociation, which is the rate-limiting step (Hackney, 1988; Hackney et al., 1989). A six-state mechanism was proposed by Sadhu and Taylor (1992) based on measurements of the rate constants of nucleotide binding using the fluorescent substrate analogs, methylanthraniloyl ATP (mant-ATP) and mant-ADP,[1] on the rate constant of dissociation of mant-ADP and on measurements of the rate constant of the hydrolysis step (the phosphate burst). The mechanism is different from myosin in that the rate of phosphate dissociation is much larger than the rate of ADP dissociation. Also the ADP affinity is extremely high, greater than 10^8 M^{-1}, based on kinetic measurements of the rate constants of association and dissociation.

The ATPase activity is increased more than 1000-fold by binding to microtubules (Kuznetsov & Gelfand, 1986). Quantitative studies of the kinetic mechanism of the microtubule−kinesin complex have proved difficult because only a fraction of the kinesin (25−40%) is activated by microtubules (Hackney, 1988; Hackney et al., 1992; Sadhu & Taylor, 1991) and the light chains of the tetramer appear to be inhibitory. It might be expected that binding to microtubules would increase the rate constant of ADP dissociation, and although the rate was increased, the value was not large enough to account for the turnover rate, and only a fraction of the kinesin gave the increase in rate (Hackney, 1988).

Chymotryptic digestion yields a fragment of about 45 kDa, which has a much larger microtubule-activated ATPase than the whole molecule (Kuznetsov et al., 1989) and a larger rate of ADP dissociation from the microtubule−kinesin−ADP complex. This fragment corresponds in size to a single head motor domain.

The expression of the motor domain in a bacterial system allows much larger quantities of protein to be obtained for kinetic studies. The motor domain of *Drosophila* kinesin consisting of the first 401 amino acids has been expressed by Gilbert and Johnson (1993, 1994), termed K401, and a construct of the first 340 or 392 amino acids, termed DKH340 and DKH392, was prepared by Hackney and collaborators (Huang & Hackney, 1994; Huang et al., 1994; Hackney, 1994). These proteins are similar to intact kinesin in having a low ATPase activity, and ADP dissociation is the rate-limiting step. Activation of the ATPase by microtubules is at least 1000-fold. Transient kinetic studies of ATP hydrolysis by the kinesin−microtubule complex were

† This work was supported by Program Project Grant HL 20592 from the National Heart Lung and Blood Institute, National Institutes of Health.

® Abstract published in *Advance ACS Abstracts,* September 15, 1995.

[1] Abbreviations: AMPPNP, 5′-adenylyl imidodiphosphate; DTT, dithiothreitol; EGTA, ethylene glycol bis(β-aminoethyl ether)-*N,N,N′,N′*-tetraacetic acid; mant-ATP and mant-ADP, 2′(3′)-*O*-(*N*-methylanthraniloyl)adenosine 5′-triphosphate and -diphosphate, respectively; mant dATP 2′-deoxy, 3′-*O*-(*N*-methylanthraniloyl)adenosine 5′-triphosphate; PIPES, 1,4-piperazinediethanesulfonic acid; PMSF, phenylmethanesulfonyl fluoride; TAME, N_α-*p*-tosyl-L-arginine methyl ester.

0006-2960/95/0434-13233$09.00/0

fitted to a four-step mechanism, which was consistent with product dissociation as the rate-limiting step (Gilbert & Johnson, 1994), although a different interpretation was proposed in Gilbert et al. (1995).

In this work, the mechanism of a human kinesin motor domain is described. The construct named K379 consists of the first 379 amino acids. In terms of alignment of the sequence at the C terminal end, K379 corresponds to a *Drosophila* construct of 387 amino acids. The results of transient kinetic experiments fit the same reaction mechanism as for the whole protein from calf brain, and the values of the rate constants of the nucleotide binding and dissociation steps and of the hydrolysis step are essentially the same as those reported in our previous study of the whole protein (Sadhu & Taylor, 1992). The results establish the suitability of the protein expressed in bacteria for the study of the kinesin mechanism.

In order to determine the mechanism of activation by microtubules, it is first necessary to determine the rate and equilibrium constants for the reaction of kinesin alone. In the accompanying paper, the reaction mechanism of the microtubule−kinesin complex is described (Ma & Taylor, 1995).

EXPERIMENTAL PROCEDURES

Expression and Purification of Human Kinesin 379. *Escherichia coli* BL21 (DE3) cells were transformed with a pET plasmid containing the truncated kinesin gene and used for expression of K379 protein. We are indebted to John Kull for the gift of this construct and for providing us with a description of his method of purification of kinesin prior to its publication. The construct was prepared from the human cDNA clone of Navone et al. (1992), which was obtained from a placenta cDNA library. Cells were grown for about 6 h with shaking at 37 °C in 25 mL of LB medium (10 g of tryptone, 5 g of yeast extract, and 10 g of NaCl/L) supplemented with ampicillin (0.1 mg/mL), washed by centrifugation three times with fresh LB plus ampicillin, and used to inoculate two 1-L volumes of fresh LB supplemented with ampicillin. The cultures were shaken at 33 °C overnight, harvested by centrifugation, and resuspended in 100 mL of lysis buffer (25 mM PIPES, pH 6.8, 0.2 mg/mL TAME, 0.005 mg/mL leupeptin, 0.005 mg/mL pepstatin A, 0.5 mM PMSF, and 2 mM DTT), and 25 μg/mL DNase I was added before lysing in a French Press. The lysate was centrifuged (SS-34 rotor, 18 000 rpm, 1 h) to remove insoluble materials. Approximately 1100 mg of protein was obtained from 2 L of cells.

The K379 was purified by chromatography on a 30-mL Whatman cellulose phosphate P11 column equilibrated with 25 mM PIPES, pH 6.8, and 75 mM NaCl. The column was washed with the same buffer to remove unbound proteins, and the K379 was eluted by a 350-mL gradient from 75 to 1000 mM NaCl in 25 mM PIPES buffer, pH 6.8. To each fraction, 2 mM $MgCl_2$ was added as soon as it was eluted from the column. The peak fractions (eluting at approximately 400 mM NaCl) were pooled and dialyzed against buffer (25 mM imidazole, pH 6.8, 75 mM NaCl, and 1 mM $MgCl_2$). The dialysate was clarified by centrifugation and applied to a 10-mL Bio-Rad Macro-Prep 50 Q column and washed with 75 mM NaCl buffer. K379 was eluted with a 130-mL gradient of 75−1000 mM NaCl in 25 mM imidazole, pH 6.8, and 1 mM $MgCl_2$. ATP was added to the pooled fractions at a ratio of 1:1 to K379. The protein was dialyzed overnight against the standard buffer used in all experiments (25 mM PIPES, pH 6.8, 2 mM $MgCl_2$, and 1 mM DTT), plus 75 mM NaCl and 2 μM ATP and then clarified. Sucrose (10% final concentration) was added, and the solutions was stored at −80 °C. The yield of kinesin was about 40 mg from 1100 mg of crude protein.

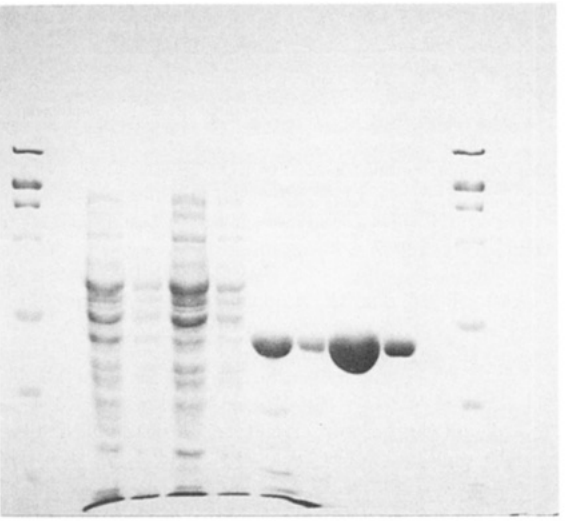

FIGURE 1: SDS−PAGE patterns to illustrate the steps in purification of K379. Lane 1, molecular weight standards; lanes 2 and 3, supernatant from sedimentation of crude lysate for 1 h at 18 K. The second lane of each pair is a 5-fold dilution of the same sample. Lanes 4 and 5, flow through from PC column; lanes 6 and 7, pooled fractions of K379 peak from PC column, dialyzed against 75 mM NaCl and clarified; lanes 8 and 9, pooled fractions of K379 peak from Q column; lane 10, molecular weight standards. Sharp band at bottom of gels in lanes 2−7 is a dye marker; 10% Laemmli gels.

More than a dozen K379 preparations were used in this work, and there was some variations in yield and purity. Figure 1 shows SDS−PAGE patterns for the steps in purification. The peak eluted from the Q column is essentially pure. Faint bands on the highly overloaded gel, which do not reproduce in the photograph, make up at most 5% of the total. In a few preparations, additional bands were detected at about 35 and 15 kDa. These appear to be generated by proteolysis of K379 during the preparation. These bands eluted with the K379 peak on gel filtration on a Sepharose 6B column (55 cm length). Partial digestion of K379 with subtilisin yields bands in the same molecular weight range that also migrate with the K379 peak on gel filtration. The contamination was avoided by discarding the initial part of the peak eluted from the PC column.

All preparations used in this work were at least 90% pure based on SDS−PAGE. In the presence of 1 mM AMPPNP, at least 90% of the protein sedimented with microtubules. The ability to bind to microtubules does not prove that the K379 is fully active since protein that had lost the nucleotide binding site might still bind to microtubules.

The content of nucleotide binding sites was determined by dialysis or a centrifuge column assay. [^{3}H]ATP was added in a 1:1 ratio to K379, and the solution was dialyzed overnight against 20 volumes of buffer containing the same concentration of [^{3}H]ATP. For the column assay, a 20-fold excess of labeled ATP was added, and the solution was incubated for 30 min−1 h at room temperature. The

solution was cooled on ice, and a 0.3-mL aliquot of the solution was layered on a 3-mL bed volume of Sephadex G-50 fine column, which had been spun for 2 min at low speed in a clinical centrifuge. The column was spun at the same speed and for the same time interval to remove the protein−nucleotide complex, and it was washed once by spinning with a 0.3-mL aliquot of buffer. All steps were done at 4 °C.

Both methods gave a content of nucleotide binding sites of 0.7−0.8 mol/mol of total protein (molecular mass of 42 kDa) or 0.8−0.9 sites/mol corrected for impurities. Since the protein initially had ADP bound, the maximum value for exchange at a 20-fold ratio is 0.95. The protein concentration was measured by Bio-Rad protein assay reagent using calibration curves prepared with bovine serum albumin or myosin subfragment 1. The content of mant-ATP binding sites was the same as ATP sites as measured by dialysis and assayed using the fluorescence emission after displacement of bound mant-ATP or mant-ADP from K379 with excess ATP.

At salt concentrations less than 50 mM, the protein slowly aggregated. All experiments were done at salt concentrations of 50 mM or larger, and the protein was stored in 75 mM NaCl.

ATPase Assays and Preparation of Nucleotides. The ATPase activity was determined by measuring the hydrolysis of [γ-^{32}P]ATP. [^{32}P]Pi produced by hydrolysis was separated from unreacted nucleotide on charcoal columns, and the fractional hydrolysis relative to total counts was measured as described previously (Sadhu & Taylor, 1992). The 2′-(3′)-*O*-(*N*-methylanthraniloyl)-ATP and -ADP were prepared from ATP and ADP by the method of Hiratsuka (1983). Several preparations were made during the course of this work. For earlier experiments, the nucleotide was purified by chromatography on Sephadex LH-20 according to the method of Hiratsuka. It was found in some cases that the purified nucleotide contained a second fluorescent component that was not completely displaced from kinesin or myosin subfragment 1 by excess ATP. This component was separated from mant-ATP by chromatography on a DEAE Sephacel column eluted with a triethylammonium bicarbonate gradient (10 mM−0.8 M). Later preparations were purified on DEAE Sephacel. The additional component appears to be the 2′,3′-bis mant-ATP based on an A_{256}/A_{356} ratio of 2.65 compared to 4.0 for the main component (Moore & Lehman, 1994). A preparation of the 3′ isomer was made by starting with 2′-deoxy-ATP. It yielded a single peak on purification by chromatography on DEAE Sephacel. The purity of the various samples was checked by thin-layer chromatography (1-propanol/NH_4OH/H_2O, 6:3:1 by volume plus 0.5 g/L EDTA and 2-propanol/H_2O/HCl, 65:18.4:11.6 on silica plates). [γ-^{32}P]mant-ATP was prepared from mant-ATP by the method of Glynn and Chapell (1964) and used for phosphate burst and some steady-state measurements. Steady-state mant-ATPase activity was determined using the Malachite green method (Lanzetta et al., 1979).

Preparation of Nucleotide-Free Kinesin. Measurements of the rates of nucleotide binding and the phosphate burst require the preparation of nucleotide-free K379 at a relatively high protein concentration. The extremely strongly bound ADP can be removed by chelating Mg with EDTA, but it was found in previous studies with brain kinesin that roughly half of the nucleotide binding sites were lost by this treatment (Sadhu & Taylor, 1992). A similar result was obtained with K379.

K379 was bound to a phosphocellulose column (2 mL of column volume/2 mL of protein solution at a concentration of 2 mg/mL) equilibrated with the standard buffer minus $MgCl_2$ and supplemented with 50 mM NaCl, 2 mM EDTA, and 0.05% Tween-20 at 4 °C. The column was washed with 20 mL of the same solution, which quantitatively removed the bound nucleotide, and the protein was eluted with high salt buffer (25 mM PIPES, 550 mM NaCl, 2 mM $MgCl_2$, 20% glycerol, and 1 mM EGTA, pH 6.9). The protein was concentrated by centrifugation using an Amicon Centriprep concentrator. This step required 1.5 h to complete. The protein was kept at high ionic strength and diluted to a lower salt concentration at the beginning of the experiments, which were begun within 2−3 h after removal of nucleotide.

The content of nucleotide binding sites was determined by the addition of [^{3}H]ATP and assayed by the centrifuge column method. The fraction of binding sites per mole of K379 was reduced from a value of 0.8−0.9 before treatment to a value of 0.45−0.5.

The loss of binding activity appeared to depend on two effects. There is some loss of sites during the short period that the protein is kept in the absence of Mg. There was a 10−15% loss of binding sites assayed immediately after elution. The addition of nucleotide and a repeat of the procedure to remove nucleotide reduced the content of sites by an additional 10% at most. The content of binding sites for mant-ATP determined by fluorescence titration of binding sites immediately after the removal of the ADP was also 0.7. However, there is an additional loss of binding activity over a 3-h period at 4 °C. The nucleotide-free protein was stable at −20 °C in the high salt−glycerol−Mg buffer for a couple of days.

The loss of sites was at least partly reversible. [^{3}H]ATP was added in small excess over the K379 concentration, and the binding was measured by the centrifuge column method as a function of time. Over a 2-h period at room temperature, the site content increased to about 80% of its initial value before the nucleotide removal step. Removal of nucleotide increases the tendency of the protein to slowly aggregate, and the salt concentration had to be kept above 100 mM. The reversible loss of binding activity might be caused by self-association of the nucleotide-free protein, which is reversed by rebinding of nucleotide. The time scale of this reversal process is very long compared to the time course of transient experiments.

Bound nucleotide can also be removed by treatment with apyrase in standard buffer (Sigma, Grade VII, 1 unit/mL). The reaction was followed by measuring the decrease in fluorescence enhancement of a K379−mant-ADP complex. The nucleotide was essentially completely dissociated in 20 min at 20 °C. Readdition of excess mant-ATP at the end of this period gave nearly complete recovery of fluorescence enhancement.

Molecular Weight of K379. The *Drosophila* construct DKH392 was shown by Huang et al. (1994) to be a dimer. Some preliminary measurements were made on K379 since it lacks only five amino acids at the C terminal end compared to DKH392, and it might also be expected to be a dimer. The molecular mass was estimated by gel filtration on

Sepharose CL 6B (55 cm column) and Sephacryl 300 superfine (85 cm column). The columns were calibrated using Bio-Rad molecular mass standards, carbonic anhydrase (29 kDa), bovine serum albumin (66 kDa), alcohol dehydrogenase (150 kDa), β-amylase (200 kDa), apoferritin (443 kDa), and Blue Dextran. Measurements on four preparations in 100 mM NaCl gave values of 90−120 kDa. The molecular mass was also measured by equilibrium ultracentrifugation using the Beckman Optima XL-A ultracentrifuge. Values of 93 and 91 kDa were obtained in 50 and 100 mM NaCl (0.15−0.42 mg/mL of K379, 13 000 rpm, 10 °C). However, the fitting program for a self-associating system had to be used to fit the concentration profile. The preliminary results agree with Huang et al. that the protein is present mainly as a dimer in 100 mM NaCl. In 150 mM NaCl, the average molecular mass was significantly smaller. Values of 60 and 70 kDa were obtained, but the result depended on the choice of constraints used in the fitting program. Some dissociation of the dimer may occur at very high ionic strength, but this aspect of the system was not investigated in the present work.

Transient Kinetic Measurements. Stopped flow and chemical quench flow measurements were made as described previously (Sadhu & Taylor, 1992) except that a Kintec Instruments mixing chamber was used in some of the more recent quench flow experiments. Slow reactions of mant-ADP or mant-ATP were measured with a Perkin Elmer MPF 44A fluorimeter (excitation, 365 nm; emission, 440 nm; the same wavelengths were used in stopped flow experiments).

Analysis of Kinetic Data. (a) Binding of mant-ADP. The fluorescence transient for the binding of mant-ADP fitted two exponential terms

$$F = L + M\exp(-\lambda_1 t) + N\exp(-\lambda_2 t)$$

where F is the increase in fluorescence emission relative to free nucleotide. The coefficients L, M, and N and the two apparent rate constants were obtained by fitting the transient using the KINFIT program (OLIS).

The simplest mechanism that can account for the results is

$$K + D \overset{K_a}{\rightleftharpoons} K(D) \overset{k_b}{\rightleftharpoons} K{\cdot}D_1 \overset{k_c}{\rightleftharpoons} K{\cdot}D_2$$

where the first step is a rapid equilibrium with association constant K_a followed by two first-order steps (isomerizations) with rate constants k_b and k_c. The transients showed an increase followed by a decrease in fluorescence, and the fluorescence emission is larger for $K{\cdot}D_1$ than for $K{\cdot}D_2$. The general solution is given in Benson (1960), and the solution for this mechanism is given in Trybus and Taylor (1981). The observed rate constants are $\lambda_1 = K_a k_b[D]/(K_a[D] + 1)$ and $\lambda_2 = k_c$ for the case that reversal of steps b and c can be neglected. The coefficients normalized to a final value of $L = 1$ are $M = (f\lambda_1 - k_c)/(k_c - \lambda_1)$ and $N = \lambda_1(1 - f)/(k_c - \lambda_1)$ where f is the ratio of fluorescence emission of $K{\cdot}D_1$ to $K{\cdot}D_2$. The coefficient M of the λ_1 term is zero for $\lambda_1 = k_c/f$.

(b) Hydrolysis Mechanism. The data was fitted to the simplest scheme for binding, hydrolysis, and release of products (Scheme 1)

Scheme 1

$$K + T \overset{K_1}{\rightleftharpoons} K(T) \overset{k_2}{\rightleftharpoons} K{\cdot}T \overset{k_3}{\rightleftharpoons} K{\cdot}DP \overset{k_4(-P)}{\Longleftrightarrow} K{\cdot}D \overset{k^d}{\rightleftharpoons} K + D$$

where T, D, and P refer to nucleotide triphosphate, nucleotide diphosphate, and inorganic phosphate, respectively. It is shown that the maximum steady-state rate k_{cat} is determined by the very small rate constant of ADP dissociation; therefore, $k_{cat} = k^d$ and at the end of the transient the system is essentially in the K·D state. The reversal of steps 2−4 can be neglected, and the transient phase in the general case fits three exponential terms with rate constants $\lambda_1 = K_1 k_2[T]/(K_1[T] + 1)$, k_3, and k_4. The fluorescence transient fitted two exponential terms, an increase followed by a decrease. The assignment of the fluorescence changes to the steps in the mechanism are discussed in the Conclusions. Simulation of the mechanisms were done using the KINSIM program of C. Freiden and B. Barshop as modified for the Macintosh by D. Wachsstock and T. Pollard.

RESULTS

ATPase Activity and Rate of ADP Dissociation. The steady-state ATPase of K379 in the absence of microtubules was 0.008 s^{-1} at 20 °C, which is roughly twice the value for native kinesin (Vale et al., 1985; Kuznetsov & Gelfand, 1986; Hackney et al., 1988; Sadhu & Taylor, 1992). The constructs of *Drosophila* kinesin have ATPase activities of 0.005 s^{-1} or less (Gilbert & Johnson, 1993; Huang & Hackney, 1994; Hackney, 1994), and ADP dissociation is the rate-limiting step.

The rate of dissociation of mant-ADP was measured by the decrease in fluorescence enhancement on the addition of excess MgATP. The K379−mant-ADP complex was formed by adding a 20-fold excess of mant-ATP to the protein, incubating for 30 min at room temperature, and removing unbound mant-ADP by the centrifuge column method. The fluorescence emission of mant-ADP bound to K379 is approximately 1.8 times the emission of free mant-ADP. The dissociation is very slow, and the reaction was measured in a fluorimeter. The decrease in fluorescence fitted one exponential with a rate constant 0.006 s^{-1} (Figure 2). The rate of hydrolysis with mant-ATP as substrate was also 0.006 s^{-1}, thus mant-ADP release is the rate-limiting step for K379 mant-ATPase. The rate of fluorescence enhancement for the binding of excess mant-ATP to K379 ADP gave a rate constant of ADP dissociation of 0.01 s^{-1} (data not shown).

Nucleotide Binding. The binding of mant-ATP and mant-ADP was investigated by measuring the enhancement of fluorescence using the stopped-flow apparatus. The signal obtained by mixing nucleotide-free kinesin with a low concentration of mant-ATP (1 μM final concentration) gave an enhancement of fluorescence that fitted a single exponential term. As the concentration was increased, the increase in fluorescence showed a small deviation from a fit to one exponential. At concentrations larger than 10 μM, the signal passed through a maximum value and then decreased as shown in Figure 3. With further increase in concentration, the maximum amplitude of fluorescence increased, but the signal decreased to the same final value.

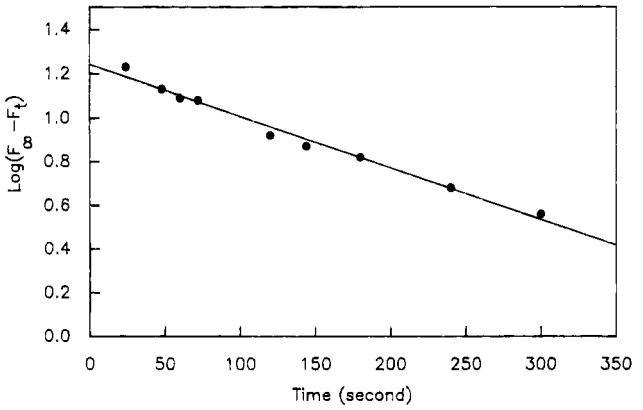

FIGURE 2: Determination of the rate constant of ADP release in the absence of microtubules. 5 μM K379 with bound mant-ADP was mixed with 50 μM ATP. The change of fluorescence enhancement was recorded using a Perkin Elmer MPF44 fluorimeter, and the rate constant was determined from a semilog plot of fluorescence change against time. The rate constant was 0.006 s^{-1}. The same rate constant was obtained with 500 μM ATP. Conditions: 25 mM PIPES, pH 6.9, 50 mM NaCl, 2 mM $MgCl_2$, and 1 mM EGTA at 22 °C.

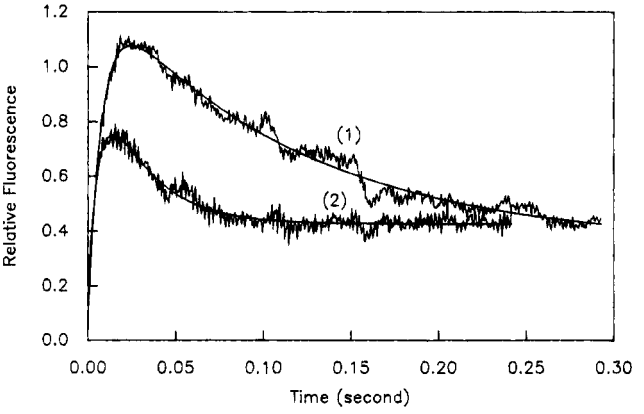

FIGURE 3: Time course of the fluorescence enhancement for the reactions of mant-ATP and mant-ADP with nucleotide-free K379. (Curve 1) 7.5 μM kinesin and 40 μM mant-ATP (concentration after mixing 1:1 in the stopped-flow apparatus). The jagged curve is the actual fluorescence signal, and the smooth curve is the computer-generated best fit to two exponential terms; rate constants 130 and 8.7 s^{-1}. (Curve 2) 7.5 μM kinesin and 40 μM mant-ADP; rate constant 150 and 38 s^{-1}. The signals were scaled to the same initial voltage to compare the amplitudes of the enhancement of fluorescence. Conditions: 20 °C, 25 mM PIPES, pH 6.9, 150 mM NaCl, 2 mM $MgCl_2$, and 1 mM EGTA.

The binding of mant-ADP showed a similar behavior, a fit to a single exponential term at very low concentrations (<3 μM) and an increase followed by a decrease at higher concentrations. The signals for mant-ATP and mant-ADP at a concentration of 40 μM nucleotide are shown in Figure 3 on a relatively long time scale to illustrate the decrease phase. The signals were normalized to the same initial voltage to show that both nucleotides gave the same final value of enhancement.

The curves were fitted to two exponential terms corresponding to the increase and decrease phases. The rate constant for the decrease phase is 10 s^{-1} for mant-ATP and 35−40 s^{-1} for mant-ADP. The larger maximum value of the fluorescence for mant-ATP compared to mant-ADP may be explained by the smaller rate of decrease, but an analysis of the mechanism is necessary to show that the high fluorescence state has the same amplitude for both nucleotides.

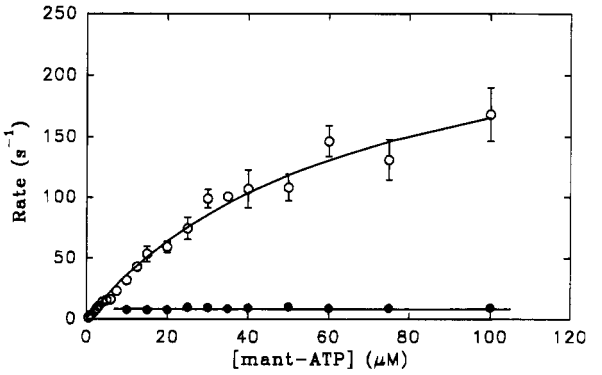

FIGURE 4: Concentration dependence of apparent rate constants for the binding of mant-ATP to nucleotide-free K379. The apparent rate constant was obtained by fitting the data to one exponential term at low substrate concentrations and to two exponential terms at high concentrations as illustrated in Figure 3. (○) Apparent rate constant for the increase in fluorescence; (●), apparent rate constant for the decrease in fluorescence. Conditions as for Figure 3, 150 mM NaCl. Bars are standard deviation of four or five measurements; bars are omitted if deviation is less than the size of the symbol. The curve for rate of increase of fluorescence was fitted to a hyperbola, maximum rate of approximately 200 s^{-1}; horizontal line is a rate constant of 9 s^{-1}. The K379 concentration was varied from 0.2 to 13 μM to maintain a ratio of substrate to accessible nucleotide binding sites of at least 5:1, except for concentrations less than 3 μM, which are at 4:1.

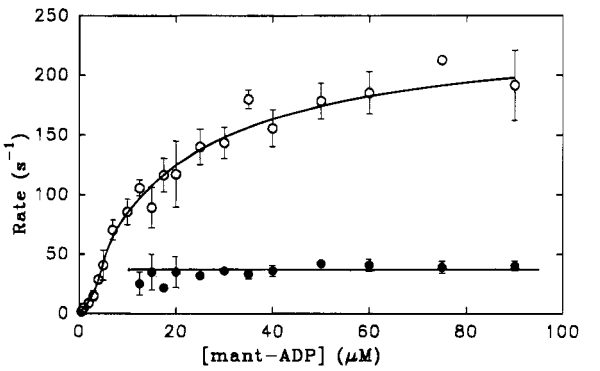

FIGURE 5: Concentration dependence of apparent rate constants for the binding of mant-ADP to nucleotide-free K379. (○) Apparent rate constant for the increase in fluorescence; (●) apparent rate constant for the decrease in fluorescence. Rising curve was fitted to an hyperbola for concentrations greater than 8 μM, maximum rate approximately 200 s^{-1}; the initial slope was obtained from a linear fit in the concentration range up to 2 μM; the horizontal line gave a rate constant of 40 s^{-1}. Conditions as for Figure 3, 150 mM NaCl. K379 concentration was varied from 0.25 to 13 μM.

The rate constants for the increase and decrease in fluorescence were determined for a range of mant-ATP and mant-ADP concentrations. Typical data sets obtained at 20 °C and 150 mM NaCl are plotted in Figures 4 and 5 for mant-ATP and mant-ADP, respectively. The rate constants showed a complex dependence on substrate concentration. For concentrations greater than 8−10 μM, the rate constant for increase in fluorescence fitted a hyperbolic dependence on substrate concentration as expected for a rapid equilibrium binding step followed by an isomerization to a state with enhanced fluorescence. The maximum rate is approximately 200 s^{-1}. The rate constant for decrease in fluorescence was essentially independent of concentration.

Measurements at very low substrate concentrations (<1 μM) have a higher noise level, but the fit to a single exponential was reproducible with an error of ±15%. The

rate constant varies linearly, and the initial slope measures the apparent second-order rate constant k^a for nucleotide binding which is 3×10^6 M^{-1} s^{-1} for mant-ATP and 5×10^6 M^{-1} s^{-1} for mant-ADP. However, the measurements deviated slightly from the hyperbola in the case of mant-ATP and markedly in the case of mant-ADP. As shown in Figure 5, the plot has an increasing slope in the range of 3−5 μM. The rate constant for increase in fluorescence rises sharply to a value of 35 s^{-1} and then follows a hyperbolic dependence on concentration.

This behavior is predicted by the simple mechanism:

$$K + D \overset{K_a}{\rightleftharpoons} K(D) \overset{k_b}{\rightleftharpoons} K{\cdot}D_1 \overset{k_c}{\rightleftharpoons} K{\cdot}D_2$$

where the first step is a rapid equilibrium with binding constant K_a followed by transitions to states with high fluorescence enhancement ($K{\cdot}D_1$) and lower fluorescence enhancement ($K{\cdot}D_2$). The fluorescence transient fits two exponential terms with observed rate constants $\lambda_1 = K_a k_b[D]/(K_a[D] + 1)$ and $\lambda_2 = k_c$ for the case that reversal of steps b and c can be neglected (see Analysis of Kinetic Data). For very low concentrations, the coefficient of the k_c term is small, and the transient fits one exponential term with rate constant $K_a k_b[D]$ where $K_a k_b$ is the apparent second-order rate constant for substrate binding. The coefficient of the λ_1 term is $(f\lambda_1 - k_c)/(k_c - \lambda_1)$ where f is the ratio of fluorescence enhancement of $K{\cdot}D_1$ to $K{\cdot}D_2$. As the concentration increases, the observed rate constant increases linearly with concentration, but the coefficient of the λ_1 term approaches zero for $\lambda_1 = k_c/f$, and the increase in fluorescence now fits a single exponential term but the rate constant is k_c, which is 35−40 s^{-1}. The value of f calculated from the ratio of coefficients obtained from fitting the transient at a high substrate concentration is 2.5−3. Consequently, the coefficient is zero for $\lambda_1 \simeq 15$ s^{-1}, which corresponds to a substrate concentration of 3−4 μM. Therefore, the simple scheme provides a quantitative explanation of the sharp increase in the observed rate constant in this concentration range.

The binding of mant-ATP also fits a mechanism in which there are two transitions to states of high and low fluorescence enhancement. The ratio of enhancements of the two states is 3, calculated from the coefficients of the fit at high substrate concentrations. Since the rate constant of the decrease phase is only 9 s^{-1}, the coefficient of the λ_1 term is zero for $\lambda_1 = 3$ s^{-1}, which corresponds to a concentration of approximately 1 μM. Measurements of the rate constant were not feasible below 0.5 μM. The initial slope of the plot in Figure 4 may be an overestimate of k^a, and only a small deviation from a hyperbola is expected in the accessible concentration range.

The mechanism provides a quantitative explanation of the dependence of rate constants on substrate concentration. However, it is necessary to consider other mechanisms that might also explain the data. mant-ATP or mant-ADP is a mixture of 2′ and 3′ isomers, which might have different affinity and different fluorescence enhancement on binding to K379, and the decrease phase of the fluorescence signal might be related to these differences. To test this possibility, the 3′ isomer was prepared from 2′-deoxy-ATP. The fluorescence signal again consisted of an increase and decrease phase; consequently, the transition in which the fluorescence decreases cannot be explained by different properties of isomers or by acyl group migration. The kinetic properties of mant-dATP are different from the mixed isomers of mant-ATP (Table 1). The maximum rate of the fluorescence increase is smaller, and although the decrease phase has the same rate of 10 s^{-1}, the amplitude of the decrease is much larger so that in the steady state the increase in fluorescence is less than 5% relative to free nucleotide. The binding of mant-dADP also gave less than a 5% increase in fluorescence. The very small enhancement is not explained by dissociation of mant-dADP in the hydrolysis reaction or the failure of mant-dADP to bind. The binding site is occupied by mant-dADP because the addition of mant-ATP gave only a slow increase in fluorescence from displacement of mant-dADP.

Table 1: Kinetic Constants for Binding of mant-ATP and mant-ADP to Kinesin K379[a]

	ionic strength NaCl (mM)	k^a (M^{-1} s^{-1})	r_2 (s^{-1})	r_3 (s^{-1})
mant-ATP	50	6×10^6	200 ± 15	9 ± 1
	150	3×10^6	200 ± 15	9 ± 1
mant-dATP	150	1.5×10^6	170	8 ± 1
mant-ADP	50	10×10^6	260 ± 20	40 ± 2
	150	5×10^6	200 ± 10	40 ± 1

[a] Data are fitted to a rapid equilibrium binding step followed by two steps in sequence:

$$K + L \overset{K_1}{\rightleftharpoons} K(L) \overset{r_2}{\rightleftharpoons} K{\cdot}L^{**} \overset{r_3}{\rightleftharpoons} K{\cdot}L^{*}$$

where L is the nucleotide ligand and asterisks refer to states of high (**) and low (*) fluorescence enhancement; k^a, the apparent second-order rate constant of nucleotide binding, is the initial slope of the plot of rate constant versus substrate concentration; r_2 is the maximum rate for the increase in fluorescence obtained by extrapolation by fitting to an hyperbola, limits refer to the range for different experiments and preparations; r_3 is the rate constant for the decrease in fluorescence, which is constant over the higher range of concentrations. mant-dATP is the 3′-*N*-methylanthraniloyl derivative prepared from 2′-deoxy-ATP. Data for mant-dATP are from one preparation. Conditions: 25 mM PIPES buffer, pH 6.9, at 20 °C, 2 mM $MgCl_2$, and 1 mM EGTA.

A second possibility is that the nucleotide binds at some other nonspecific site through the methyl anthranylate ring and the binding at the ATP site might reduce the fluorescence or the affinity at this site. The content of binding sites measured by dialysis was not larger for mant-ADP than for [^{3}H]ADP, and for dialysis experiments at high concentrations of K379, the free nucleotide concentration was 20 μM, which is more than 1000 times larger than the dissociation constant at the specific site. Thus, there is no evidence for a weaker site with dissociation constant in the 20 μM range. In a single turnover experiment with K379 in excess over mant-ATP, the fluorescence showed an increase and decrease phase while binding is expected to be limited to the high affinity site in this case.

The addition of increasing amounts of ATP to nucleotide-free K379 simply reduced the amplitude of the fluorescence transient, but the time course was unchanged. The treatment of K379 to remove bound nucleotide does lead to the loss of nucleotide binding site over a period of time. However, removal of bound nucleotide by treatment with apyrase for 20 min followed by reaction with excess mant-ATP gave complete recovery of bound nucleotide and a biphasic fluorescence transient.

There is no evidence in favor of a second site. The rate constant of fluorescence decrease is different for mant-ADP

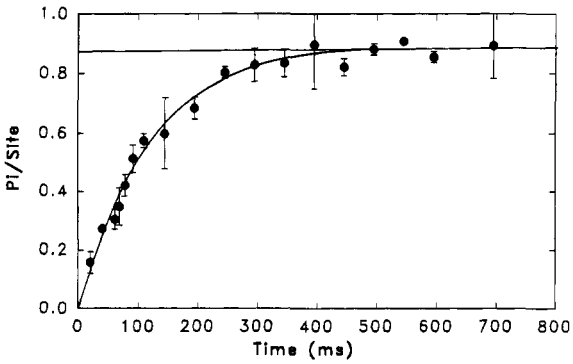

FIGURE 6: Phosphate burst phase of K379. Measurements were made in a quench flow apparatus for times up to 700 ms. The steady-state rate was also measured over the time period 5−20 s. The bars are the range for two or three measurements. Data are fitted to one exponential plus a linear term, $P_i = B(1 - \exp(-kt) + V_s t$ using simplex method (PSI plot program), $k = 8.4\ s^{-1}$, B (burst) = 0.88, V_s (steady-state rate per site) = $0.021\ s^{-1}$. Steady-state rate over long times was also $0.02\ s^{-1}$. Data are expressed relative to content of nucleotide binding sites measured on the same sample by centrifuge column method. Conditions: 25 mM PIPES buffer, pH 6.9, 2 mM $MgCl_2$, 1 mM EGTA, 75 mM NaCl, 12 μM K379, 50 μM ATP, and 6 μM site concentration at 20 °C.

and mant-ATP, and the rate constant of the decrease phase for mant-ATP is larger for the microtubule−K379 complex (Ma & Taylor, 1995). The evidence supports the interpretation that the decrease in fluorescence measures a first-order (isomerization) step in the reaction. The rate constants for nucleotide binding are given in Table 1.

Phosphate Burst Phase. The rate of the hydrolysis transient phase is relatively small. The results of an experiment are shown in Figure 6 (50 μM ATP, 12 μM protein, and 75 mM NaCl in standard buffer). The formation of phosphate is expressed relative to the content of ATP binding sites measured at the beginning of the experiment by the centrifuge column method. The data, fitted to an exponential plus a linear term, gave a rate constant of 8.4 s^{-1}, a burst of 0.88 phosphate per accessible nucleotide site, and a steady-state rate of $0.02\ s^{-1}$. The actual nucleotide site content is 0.5 per K379 in this experiment. The steady-state rate, which is the slope of the linear phase, is not determined accurately because the line is nearly horizontal in this time range. Separate measurements of the steady-state rate over the 5−20-s time range were included with each transient experiment. The rate in this experiment was $0.02\ s^{-1}$ expressed per nucleotide binding site.

The rate constant of the burst at an ATP concentration of 20 μM was $8\ s^{-1}$. Therefore, the observed rate constant has reached a maximum value at 50 μM, which is the rate constant of the hydrolysis step in the kinetic scheme (k_3).

The rate constant was measured for a range of ionic strengths. Values for NaCl concentrations of 50, 75, and 150 mM in standard buffer are 10, 8.5, and $8\ s^{-1}$. The difference is not larger than the experimental error. It is concluded that the hydrolysis step has very little dependence on ionic strength and the rate constant of the hydrolysis step is $9 \pm 1\ s^{-1}$.

Stoichiometry of Phosphate Burst. The phosphate burst is close to 1 per available nucleotide binding site. If the K379 concentration is in excess over the ATP concentration, the ATP is essentially completely hydrolyzed in a few seconds (95% or greater). The same result was obtained for brain kinesin. Either the rate of reversal of the hydrolysis step is small compared to the forward rate constant or the rate of dissociation of phosphate is large compared to the rate of reversal of the hydrolysis step or both.

The actual burst size was only 0.4−0.6 per K379 in various experiments, which was attributed to the loss of accessible binding sites with time because the nucleotide-free protein is unstable. Because K379 forms a dimer, it could be argued that only one site per dimer is active. To test this possibility, the bound nucleotide was removed by treatment with apyrase for 20 min, and the size of the phosphate burst was measured immediately. The size was 0.8−0.9 mol/mol of K379 in 150 mM NaCl. The correction for hydrolysis of ATP by apyrase in the time range up to 2 s was less than 10%. The nucleotide-free K379 prepared by apyrase treatment also slowly aggregated with loss of binding activity.

CONCLUSIONS

The human kinesin motor domain K379 expressed in bacteria has essentially the same kinetic properties as the whole tetrameric protein isolated from brain. The apparent second-order rate constants for mant-ATP and mant-ADP binding agree within a factor of 2 with the previous results, and the maximum rate of fluorescence enhancement and the rate of the phosphate burst are not significantly different from the previous values obtained for the brain protein by Sadhu and Taylor (1992). An additional isomerization step was detected for mant-ADP binding, probably because the previous measurements were not extended to a sufficiently high nucleotide concentration. The ATPase activity of K379 is activated more than 2000-fold by microtubules (Ma & Taylor, 1995). The motor domain expressed in bacteria therefore provides a satisfactory system for studies of the mechanism.

Kinetic Mechanism of K379. The data for the hydrolysis reaction fits Scheme 1, where T, D, and P refer to nucleotide triphosphate, nucleotide diphosphate, and inorganic phosphate, respectively. The constant k^d is the effective rate constant of ADP dissociation, which is equal to the maximum rate of hydrolysis (k_{cat}). The binding of mant-ADP is described by Scheme 2

Scheme 2

$$K + D \overset{K_a}{\rightleftharpoons} K(D) \overset{k_b}{\rightleftharpoons} K{\cdot}D_1 \overset{k_c}{\rightleftharpoons} K{\cdot}D_2$$

where the states $K{\cdot}D_1$ and $K{\cdot}D_2$ have high and low enhancement of fluorescence, respectively.

The rate constants for the isomerization steps k_2 and k_b were measured only for mant-ATP and mant-ADP. However, mant-ATP and mant-ADP appear to be satisfactory analogs of the normal substrates. The values of k_{cat} agree within 20%, and dissociation of mant-ADP is also the rate-limiting step for mant-ATPase. It is shown for microtubule−K379 that ATP and mant-ATP have similar values for the rate of hydrolysis step, the nucleotide diphosphate dissociation step, and the maximum rate of microtubule-activated hydrolysis (Ma & Taylor, 1995).

The initial step in binding of mant-ATP and mant-ADP is a rapid equilibrium step since the apparent second-order rate constant is much smaller than expected for a diffusion-controlled reaction. The second step is an isomerization with a rate constant of approximately $200\ s^{-1}$ for both nucleotides. The enhancement of fluorescence of $K{\cdot}T$ and $K{\cdot}D_1$ is

approximately the same based on the coefficients of the fit of the transient to two exponential terms. The fluorescence enhancement decreases to the same final value for both reactions. In the steady-state hydrolysis reaction, the system is almost completely in the K·D state while the very large binding constant of mant-ADP is consistent with $K{\cdot}D_2$ being the main state present at equilibrium. The rate constant of dissociation of mant-ADP is the same for both reactions. Therefore, K·D and $K{\cdot}D_2$ appear to be the same intermediate.

In the hydrolysis reaction, the state of high fluorescence enhancement (K·T) is converted to a state of low enhancement (K·D) at a rate of 10 s^{-1}. In the binding of mant-ADP, the high fluorescence state ($K{\cdot}D_1$) is converted to the same low fluorescence state K·D with a rate constant of 40 s^{-1}. Since the rate constant of the hydrolysis step is 9 ± 1 s^{-1}, the decrease in fluorescence could occur at the hydrolysis step or a step that rate limits the hydrolysis step. However, the decrease could also occur for the transition from K·D·P to K·D if the rate constant for this step is larger than the rate constant of the hydrolysis step since the fluorescence change would be rate limited by hydrolysis. Similar results were obtained for brain kinesin by Sadhu and Taylor (1992), who concluded that either alternative would fit the data. The second explanation is preferred for two reasons. First, in the corresponding reaction of the microtubule−K379 complex, the rate constant of the hydrolysis step is more than two times larger than the rate constant of decrease in fluorescence (Ma & Taylor, 1995), which indicates that the fluorescence change does not occur in the hydrolysis step. Second, the smaller rate constant for the decrease in fluorescence in the hydrolysis reaction compared to the reaction with mant-ADP is consistent with the rate of decrease being limited by the rate of hydrolysis.

Changes in fluorescence emission of bound mant nucleotides have been correlated with hydrolysis or phosphate dissociation steps for other enzymes. Woodward et al. (1991) reported at 10% decrease in fluorescence for the transition from the myosin−mant-ADP−phosphate intermediate to the myosin−mant-ADP state. An 8−10% decrease in fluorescence emission occurs for the hydrolysis of bound mant-GTP by p21 ras (Moore et al., 1993).

A set of constant for Scheme 1 for 50 mM salt and 20 °C is

$$K + T \underset{}{\overset{2 \times 10^4\ M^{-1}}{\rightleftharpoons}}$$

$$K(T) \overset{200\ s^{-1}}{\rightleftharpoons} K{\cdot}T \overset{9\ s^{-1}}{\rightleftharpoons} K{\cdot}D{\cdot}P \underset{(-P)}{\overset{>9\ s^{-1}}{\rightleftharpoons}} K{\cdot}D \overset{0.01\ s^{-1}}{\rightleftharpoons}$$

$$K(D) \overset{2 \times 10^{-5} M}{\rightleftharpoons} K + D$$

The binding and dissociation constants are estimates of the values for mant-ATP and mant-ADP. The rate constant of >9 s^{-1} is based on the assignment of the decrease in fluorescence to the step or steps involved in phosphate release. Based on direct measurements of the rate of phosphate dissociation, Gilbert et al. (1995) proposed that the rate constant is greater than 13 s^{-1} for a *Drosophila* construct (K401).

Comparison of K379 and Myosin. The series of steps in Scheme 1 is the same as for myosin, but there are important differences in some of the rate constants. Nucleotide binding induces a conformation change with a rate constant of approximately 200 s^{-1} both for mant-ATP and mant-ADP. The values for myosin are 100−150 s^{-1} [Woodward et al. (1991) and unpublished observations in this laboratory]. The rate of the hydrolysis step, approximately 10 s^{-1}, is about 10 times smaller than for myosin (Johnson & Taylor, 1978). The major difference as first shown by Hackney (1988) and Hackney et al. (1989) is the very small rate of ADP dissociation compared to phosphate dissociation while the reverse is true for myosin at least at 20 °C. At 5 °C, the rates of phosphate and ADP dissociation are similar (Bagshaw & Trentham, 1974).

Problem of Interaction of Nucleotide Sites of the K379 Dimer. Preliminary measurements of the molecular weight of K379 indicated that the protein is a dimer in 100 mM NaCl in the standard buffer in agreement with the finding of Huang et al. (1994) that the *Drosophila* motor domain DKH 392 is a dimer. An interaction between the heads of a dimer may be necessary in the coupling of microtubule−kinesin ATPase to motion. An important question is whether there is an interaction between nucleotide sites in the free enzyme. A detailed comparison of the kinetic mechanisms of monomeric and dimeric kinesin constructs will be presented elsewhere. The kinetic evidence presented here is quantitatively explained by Scheme 1, which assumes that the heads are independent. Two aspects of the mechanism that might be taken as evidence for interactions are the positive curvature in the plot of the apparent rate constant of the substrate binding step (Figure 5) and a phosphate burst of only approximately 0.5 per mole of K379. The shape of the curve in Figure 5 is predicted by the kinetic scheme, and a similar dependence has been obtained for the binding of mant-ADP to K332, a monomeric construct (unpublished observations). The phosphate burst is close to 1 per mole of K379 (two per dimer) when assayed immediately after removing the free nucleotide, and the low value of the burst and the number of accessible nucleotide binding sites appear to be caused by the instability of the nucleotide-free protein.

At present, no positive evidence has been obtained for interaction between heads of the dimer, and Scheme 1 will be used as the basis for the study of microtubule activation described in the accompanying paper (Ma & Taylor, 1995).

ACKNOWLEDGMENT

We wish to thank Aldona Rukuiza for expert technical assistance, John Kull for providing the K379 construct, Dr. A. Scanu for the use of the Beckman XLA ultracentrifuge in the Shared Equipment Facility, and Dr. G. Fleiss for assistance with the measurements.

REFERENCES

Bagshaw, C. R., & Trentham, D. R. (1974) *Biochem. J. 141*, 331−349.
Benson, S. W. (1960) *Foundations of Chemical Kinetics*, p 39, McGraw Hill, New York.
Gilbert, S. P., & Johnson, K. A. (1993) *Biochemistry 32*, 4677−4684.
Gilbert, S. P., & Johnson, K. A. (1994) *Biochemistry 33*, 1951−1960.
Gilbert, S. P., Webb, M. R., Brune, M., & Johnson, K. A. (1995) *Nature (London) 373*, 671−676.
Glynn, I. M., & Chappell, J. B. (1964) *Biochem. J. 90*, 147−149.
Hackney, D. D. (1988) *Proc. Natl. Acad. Sci. U.S.A. 85*, 6314−6318.
Hackney, D. D. (1994) *J. Biol. Chem. 269*, 16508−16511.
Hackney, D. D., Levitt, D. J., & Suhan, J. (1992) *J. Biol. Chem. 267*, 8696−8701.

Hiratsuka, T. (1983) *Biochim. Biophys. Acta 742*, 496−508.
Huang, T. G., & Hackney, D. D. (1994) *J. Biol. Chem. 269*, 16493−16501.
Huang, T. G., Suhan, J., & Hackney, D. D. (1994) *J. Biol. Chem. 269*, 16502−16507.
Johnson, K. A., & Taylor, E. W. (1978) *Biochemistry 17*, 3432−3442.
Kuznetsov, S. A., & Gelfand, V. I. (1986) *Proc. Natl. Acad. Sci. U.S.A. 83*, 8530−8534.
Kuznetsov, S. A., Vaisberg, E. A., Rothwell, S. W., Murphy, D. B., & Gelfand, V. I. (1989) *J. Biol. Chem. 264*, 589−595.
Lanzetta, P. A., Alvarez, L. J., Reinach, P. S., & Candia, O. A. (1979) *Anal. Biochem. 100*, 95−97.
Ma, Y. Z., & Taylor, E. W. (1995) *Biochemistry 34*, 13242−13251.
Moore, K. J. M., & Lohman, T. M. (1994) *Biochemistry 33*, 14550−14564.
Moore, K. J. M., Webb, M. R., & Eccleston, J. F. (1993) *Biochemistry 32*, 7451−7459.
Navone, F., Niclas, J., Hom-Booher, N., Sparks, L., Burnstein, H. D., McCaffrey, G., & Vale, R. D. (1992) *J. Cell Biol. 117*, 1263−1275.
Sadhu, A., & Taylor, E. W. (1991) *Biophys. J. 59*, Abstract 567a.
Sadhu, A., & Taylor, E. W. (1992) *J. Biol. Chem. 267*, 11352−11359.
Taylor, E. W. (1991) *J. Biol. Chem. 266*, 294−302.
Trybus, K. M., & Taylor, E. W. (1982) *Biochemistry 21*, 1284−1294.
Woodward, S. K. A., Eccleston, J. F., & Geeves, M. A. (1991) *Biochemistry 30*, 422−430.

BI950518T